Study on the damage mechanics model of asphalt pavement under high temperature and the optimization design of finite element parameters - Taking Guangle Expressway as an example

X. Wang[1], Z. Zhang[1,*], Z. Zhan[1], X. Li[1] and J. Yang[1]

[1]*Guangzhou Maritime University, Guangzhou, Guangdong, 510725*
*__Corresponding author__: zhzw2018@163.com

ABSTRACT In this paper, based on the reliability of the control index APPDI under different base asphalt pavement structures, the research on the correlation analysis between the damage of asphalt pavement and the material strength under high temperature conditions is carried out. Relying on the Guangle Expressway as the project, the distribution of APPDI in the pavement structure was analyzed, and the parameters of the asphalt pavement material were optimized by adjusting the cohesion C and tensile strength σt of the pavement material, and compared with the results of the Marshall test to determine the optimal parameters of the pavement material. Safety and rationality, comprehensive experimental analysis: It is suggested that the design parameters that should be used in pavement design are cohesion of 0.1630 MPa, elastic modulus of 681.41 MPa, and Poisson's ratio of 0.35. This research can provide a new idea for the design of structural materials for asphalt pavement.

KEYWORDS APPDI indicator; Asphalt road; Finite element; Parameter optimization; Material strength

1. Introduction

In recent years, due to the increasing traffic volume and the serious deterioration of overloading phenomenon, the heavy vehicle load has appeared, making the transportation present the characteristics of high flow and heavy load. With the increase of the strength of the base layer and the increase of the thickness of the asphalt surface layer, Top-Down cracking and rutting of the asphalt pavement surface layer have become the main phenomena of asphalt pavement deterioration. This Top-Down cracking and rutting has attracted extensive attention from road workers in various countries. Strength theory is the study of the laws and calculation guidelines for the yielding and damage of materials under complex stress states (Chen and Sun, 2018). In the field of geological engineering and geotechnical engineering, the Mohr-Coulomb criterion for two-dimensional stress states (Xie et al., 2020; Li and Huang, 2017; Guo et al., 2018; Gao et al., 2021; Rukhaiyar and Samadhiya, 2018) and the Drucker-Prager criterion for three-dimensional stress states (Li, 2017; Guo et al., 2021; Sun et al., 2020; Kabwe, 2020) are the commonly used strength criteria in geotechnical elastoplastic mechanics, and are the oldest, most studied, and most widely used strength theories among various strength theories.

Schorsch (2003) concluded that segregation causes Top-Down cracks in asphalt pavements and the segregated areas are prone to fatigue cracks. Through investigation and research, it was concluded that the poor fatigue performance of the road surface was due to the high void ratio caused by insufficient compaction and thus accelerated aging. Hu (2009) used finite element analysis of Top-Down cracking, considered the changes in tire pressure and vehicle axle weight, and established a three-dimensional four-layer system finite element model to conclude that the strong shear stress under wheel load was the main cause of Top-Down cracking. Gu et al. (2012) proposed a simulated dynamic load model based on the measured tire grounding pressure for the external influencing factors (temperature and load) of rutting, and established a three-dimensional finite element model for rutting analysis based on the simulated dynamic load and temperature field distribution gradient by combining the temperature field analysis of pavement structure and material test results, and studied the development law of rutting under the actual temperature and load environment of the Beijing-Shanghai Expressway. Cong et al. (2013) analyzed the causes of asphalt pavement prone to rutting and fatigue damage under heavy load conditions, based on the theory of elastic laminar system, and studied the effects of super-heavy traffic load on asphalt pavement rutting and fatigue life by characterizing pavement rutting and fatigue life by rutting volume and shear stress, and subgrade fatigue model, respectively, using ABAQUS finite element software. The effect of heavy load on structural damage of asphalt pavement was significant, and the rutting and fatigue lesions were more severe with the increase of subgrade modulus. Xu and Wu (2013) analyzed the effect of structural layer parameters on the maximum shear stress within the asphalt layer for the commonly used semi-rigid base asphalt pavement using a theoretical calculation model of multilayer elastic laminate system, and the results showed that a reasonable combination of structural layer parameters can reduce the maximum shear stress within the asphalt layer and improve the rutting resistance

DOI: 10.52292/j.laar.2024.3134
Received: February 21, 2023.
Accepted: June 1, 2023.
Recommended by Germán Prieto.

of the asphalt pavement.

It is inaccurate to take the magnitude of tensile stress or shear stress as the control index in a single way. In this paper, the damage mechanism of the pavement structure is discussed from the way of the main stress composition form the force, and the parameter optimization design is carried out, and the suggested values of the residual material parameters of the pavement structure are proposed.

2. Asphalt Pavement Potential Damage Index

The Moore-Coulomb strength theory is one of the most widely used strength theories in mechanics. The Moore-Coulomb strength theory considers material damage as shear damage, where the shear stress τ_f at the damage surface is a function of the normal stress σ:

$$\tau_f = f(\sigma) \tag{1}$$

The curve determined by this functional relationship is called the Mohr damage envelope.

As shown in Fig.1, under static load conditions, the stress states at points A and B, which are composed in different ways but have the same magnitude of shear stress, are in a safe state, but under fatigue loading, point A will have a shorter fatigue life because it is closer to the Mohr envelope.

In the previous studies, more attention was paid to the effect of shear stress magnitude on pavement damage, and more methods of viscoelastic mechanics and fracture mechanics were used to study the generation of rutting and TOP-DOWN cracking. The study of the mechanical response of the material in the multi-axial state of the pavement surface using Mohr circle analysis of the stress state of the pavement structure, especially the way of the composition of the principal stress in the shear stress on the pavement structure, is basically absent. In order to compare the possible effects of the composition mode of principal stresses in shear stress on pavement damage, a new two-dimensional pavement structural damage index, Asphalt Pavement Potinal Damage Index (APPDI) with fatigue loading, is defined as follows:

$$\text{APPDI} = \frac{\text{radius of Mohr circle at any point } \tau\sigma}{\text{its circle center to envelope distance } O_1M}$$

where $0 < \text{APPDI} < 1$, when $\text{APPDI} \geq 1$ indicates that the pavement has reached yield damage at that location.

Assuming that the material $c-\varphi$ is known, the distance from the center point $O_1\,(x_0, y_o)$ of the Mohr circle A to the envelope $Ax_0 + By_0 + C = 0$ is given by

$$O_1M = \frac{|Ax_0 + By_0 + C|}{\sqrt{A^2 + B^2}} \tag{2}$$

where the coordinates of O_1 are $x_0 = \frac{(\sigma_1+\sigma_3)}{2}$, $y_0 = 0$; radius is:

$$\tau_{0_i} = \frac{\sigma_1 - \sigma_3}{2} \tag{3}$$

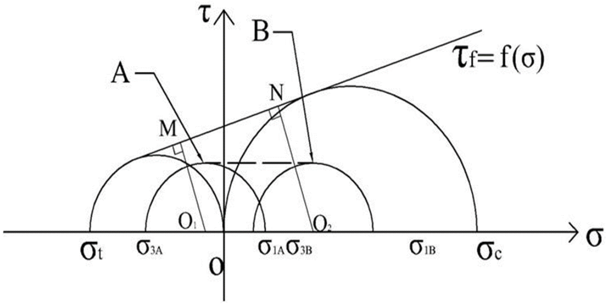

Figure 1: Mohr circle and Mohr breaking envelope.

The equation of the envelope of the material $c-\varphi$ is $\sigma \cdot \tan\varphi - \tau + c = 0$ (c, φ are known), then O_1M is:

$$O_1M = \frac{\left|\tan\varphi \cdot \frac{\sigma_1+\sigma_3}{2} - 0 + c\right|}{\sqrt{(\tan\varphi)^2 + (-1)^2}} = \frac{|\tan\varphi \cdot (\sigma_1+\sigma_3) + 2c|}{2\sqrt{\tan^2\varphi + 1}} \tag{4}$$

Combining Eq. 3 and Eq. 4, the APPDI of the stress state (σ_1, σ_2) at any point A can be calculated as:

$$\text{APPDI} = \frac{\tau_{0_i}}{O_1M} = \frac{(\sigma_1 - \sigma_3)\sqrt{\tan^2\varphi + 1}}{|\tan\varphi \cdot (\sigma_1 + \sigma_3) + 2c|} \tag{5}$$

3. Mechanics model

3.1 Pavement material parameters and geometric model

The parameters such as material name, thickness, elastic modulus, and Poisson's ratio of each layer for the finite element analysis of asphalt pavement under high temperature conditions are shown in Table 1.

The pavement structure model is simplified to a three-dimensional bicircular uniform load model, and this elastic finite element model uses 8-node 6-sided solid cells with a centrosymmetric model, and the model is determined to be 10 m long, 10 m wide, and the roadbed calculation depth is 8 m through the convergence calculation of the forces on the pavement structure. The finite element mesh model is shown in Fig. 2.

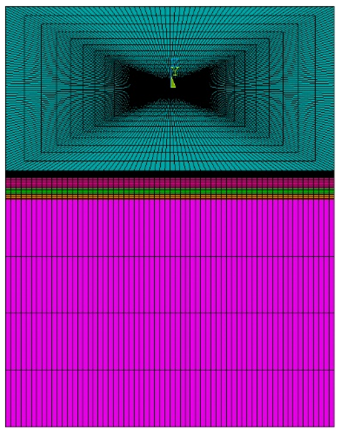

Figure 2: Three-dimensional finite element model mesh.

Table 1: Guangle Expressway asphalt pavement structure and its high temperature 60 °C material parameters.

Road surface structural layer		Material Name	H/cm	E/MPa	ν	C/MPa	φ/°
	Upper layer	Medium Grain Asphalt Concrete	4.5	350	0.35	0.0809	40
Top layer	Middle surface layer	Medium Grain Asphalt Concrete	5.5	400	0.35	0.1174	42
	Lower layer	Coarse-grained asphalt concrete asphalt gravel	7	500	0.35	0.1678	45
Upper grassroots		Graded gravel	7.5	1500	0.35	/	/
Lower grassroots		Thick cement stabilized graded gravel	36	225	0.35	/	/
Substrate		Thick cement stabilized graded gravel	20	400	0.2	/	/
Bedding layer		Graded gravel	20	200	0.2	/	/
Road base		Road base	-	35	0.4	/	/

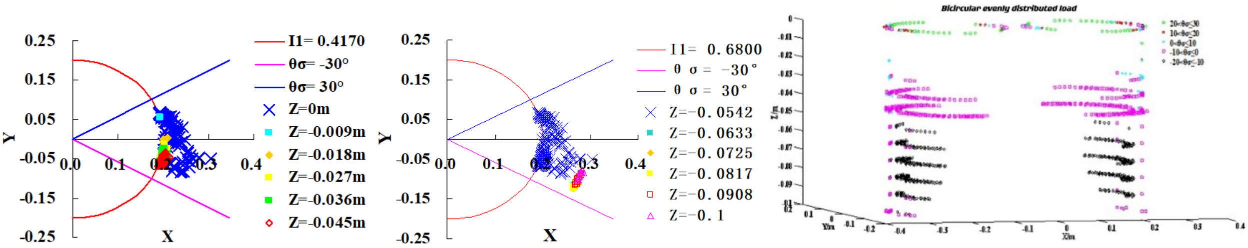

(a) Upper layer (b) Middle surface layer (c) Three-dimensional scatter plot

Figure 3: Surface π-plane projection and 3D scatter diagram.

As shown in Fig. 2, the pavement structure is finite-element calculated using the theory of elastic laminar continuous system under uniaxial bicircular uniform vertical load, the load q is 0.7 MPa, the radius of the load area of action r is 10.65 cm, and the distance between the centers of the two wheel tires is $3r$. Eight-node isoparametric cells are used for modeling. The boundary conditions are assumed as follows: the bottom surface is completely con-strained, there is no X-direction displacement on both sides in the X-direction, no Y-direction displacement on both sides in the Y-direction, and the interlayer contact state is assumed to be completely continuous. The finite element mesh model has a total of 326382 cells and 331758 nodes.

3.2 Mechanical analysis of a simplified model of bicircular uniform load for asphalt pavement damage mode

The coordinates of each node and the three principal stresses were obtained by finite element calculation under high temperature conditions. According to the defined APPDI3D, the data are calculated and processed by Matlab program to analyze the distribution of danger points and π planes for each surface layer APPDI3D > 1 in the model, as shown in Fig. 3.

Figure 3 shows that: under the bicircular uniform load model, there are 465 potential hazard points with APPDI3D greater than 1 in the upper layer, analyzed from the π-plane projection diagram, the stress composition of potential hazard points in the z-direction from $z = 0$ m to$z = -0.045$ m is a tensile-compressive composite shear stress dominated by tensile stress, where the maximum value of APPDI3D is 1.5348, $\sigma_1 = 0.0645$ MPa, $\sigma_3 = -0.0823$ MPa ,corresponding to the Lodder angle of -9.41°, located at the road surface of the outer wheel load 4 cm, $|\sigma_1| < |\sigma_3|$, the stress state is the tensile-compressive stress ratio $|\sigma_3|:|\sigma_1|$ = 1:0.78 tensile-shear stress, the possible damage mode TOP-DOWN cracking and rutting coexist. There are 449 potential hazard points with APPDI3Dgreater than 1 in the middle surface layer. From the analysis of π-plane projection diagram, the stress composition of potential hazard points in z-direction from $z = 0$ m to $z = -0.045$ m is mainly tensile-compressive compound shear stress, where the maximum value of APPDI3D is 1.0189, $\sigma_1 = 0.2852$ MPa, $\sigma_3 = 0.0085$ MPa, corresponding to the Lodder angle is -16.33°, located at the road surface of the outer wheel load 4 cm, $|\sigma_3| < |\sigma_1|$, the stress state is the tensile-compressive stress ratio $|\sigma_3|:|\sigma_1|$ = 1:33.55 compressive stress, and the possible damage mode appears as rutting.

4. Experimental analysis

4.1 Project overview

This paper is based on Guangdong Guangle Expressway, the pavement structure parameters are as follows, up and down two-way four lanes, the design speed is 120 km/h and 100 km/h. The upper layer of the main line is 4.5 cm thick GAC-16C modified asphalt concrete, the middle layer is 5.5 cm thick GAC-20C modified asphalt concrete, the lower layer is 7 cm thick GAC-25C asphalt Concrete, the upper base layer adopts 18 cm thick cement stabilized gravel, the lower base layer adopts 18 cm thick cement stabilized gravel, the bottom base layer adopts 20 cm thick cement stabilized gravel, the bedding layer adopts 15 cm graded gravel, the hard shoulder is the same as the lane requirement, the interchange ramp pavement and toll plaza adopts cement concrete pavement.

Table 2: Material parameters of asphalt top layer of Guangle Expressway under the simplified model of double-circle uniform load.

Temperature	Optimize cohesion C/MPa		$\varphi/°$	Modulus of elasticity E/MPa	APPDI Maximum	Number of danger points
60 °C	0.0809	Road surface parameters	40	350	1.5348	465
	0.1180	Optimization parameters		502.39	1.1876	27
	0.1290			546.73	1.1303	21
	0.1630			681.41	1.0689	14
	0.1800			747.48	1.0451	9
	0.2000			824.18	1.0200	7

Table 3: Marshall test parameters table.

Type	Computational Models	Modulus of elasticity/Pa	Poisson's ratio v	C/Pa	Friction angle/°
Clamps	Elasticity Model	2E11	0.3		
Simulation specimens	Elasticity Model	681.41E6	0.35	0.163E6	40

4.2 Asphalt pavement material design

The APPDI3D values of each node of the asphalt surface layer are obtained by finite element calculation, and the maximum value of APPDI3D of the upper layer is 1.5348, $\sigma_1 = 0.0645$ MPa, $\sigma_3 = -0.0823$ MPa, and the corresponding Loder angle is -9.41°. In this subsection, the material parameters of the upper layer of the asphalt pavement are optimally designed from the road performance and safety performance. Taking the tensile stress ratio and cohesion of the material as the measurement index, the cohesion of the upper layer APPDI3D < 1 in the high-temperature asphalt pavement structure is taken as the strength parameter when the tensile strength ratio of the material $|\sigma_3|:|\sigma_1| < 1:0.5$ is satisfied, and the pavement structure is in the elastic deformation stage at this time. The results of the analysis are shown in Table 2.

Table 2 shows that the cohesion (C) value of the optimized pavement material increases from 0.1180 MPa to 0.118 MPa in the high temperature case, and the modulus of elasticity E increases from 502.39 MPa to 824.18 MPa as calculated by

$$C = 2.42037 \times 10^{-8} E^2 + 2.22716 \times 10^{-4} E \tag{6}$$

The optimized modulus of elasticity is substituted into the pavement structure, and the maximum value of APPDI3D decreases with the increase of cohesion C. When $C = 0.1630$ MPa, the maximum value of APPDI3D is 1.0689, APPDI3D is close to 1, and the number of danger points in the model is 14, so $C = 0.1630$ MPa is determined as the design parameter of this pavement material.

4.3 Experimental results

The Marshall test under this parameter was simulated by ANSYS software, and the results of the numerical test were compared with the indoor test results, and the technical specification for road asphalt pavement construction was referred to further verify the reasonableness of the optimized results of the pavement structure material parameters.

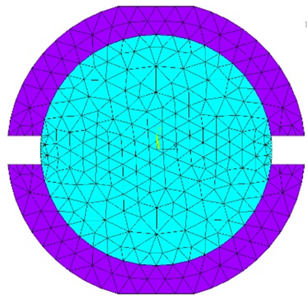

Figure 4: Marshall numerical model.

4.3.1 Marshall test parameters design and modeling

The Marshall test parameters are the structural parameters of the asphalt pavement obtained from the optimization in the previous section, and the calculated parameters of the test fixture and specimen in the ANSYS numerical simulation are shown in Table 3.

The Marshall test model is shown in Fig. 4, with a model size of 152.4 mm in diameter and 95.3 mm in height. Four sets of constant concentrated forces were applied to the specimen, 4 kN, 6 kN, 10 kN, and 13 kN. finite element analysis was performed on the specimen to obtain the three principal stresses at each node in the specimen. APPDI was used to determine the plastic state of each node in the specimen to obtain the flow value and stability of the specimen.

4.3.2 Analysis of numerical simulation results of Marshall test

When the applied load is 4 kN, the Y-direction cloud, Y-direction stress cloud and APPDI cloud of the Marshall specimen are shown in Fig. 5.

Figure 5 shows that: when the force is 4 kN, (a) the figure shows that the displacement at the top of the specimen in the Y direction is large and the displacement at the bottom is small, and the cloud is symmetrical, and the maximum displacement is 0.0038 mm; (b) the figure shows that the location where the potential danger points appear in the specimen is in the two regions A and B in the

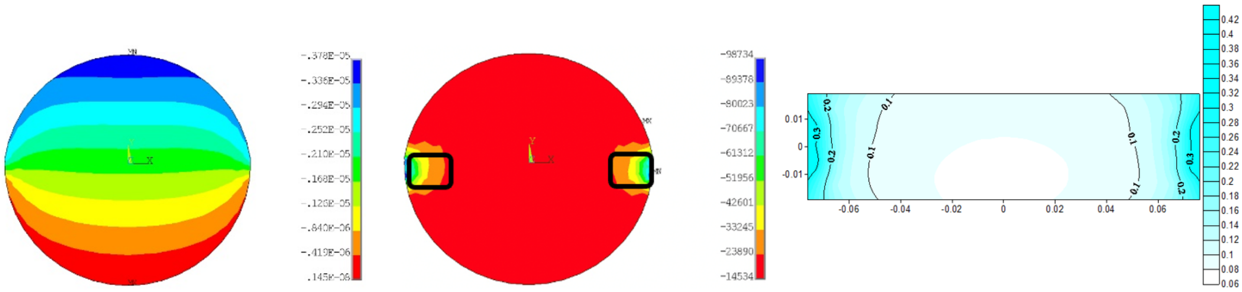

(a) Y-direction displacement cloud when the load is 4 kN

(b) Stress cloud in Y direction when the load is 4 kN

(c) APPDI3D cloud map when the load is 4 kN

Figure 5: Numerical simulation results of the specimen

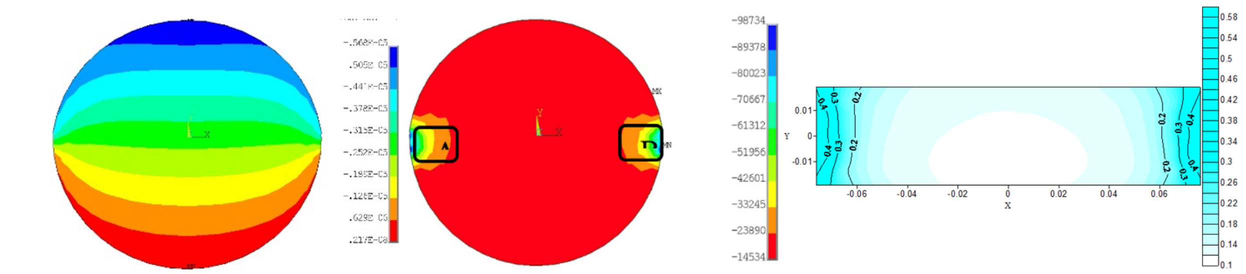

(a) Y-direction displacement cloud when the load is 6 kN

(b) Stress cloud in Y direction when the load is 6 kN

(c) APPDI3D cloud map when the load is 6 kN

Figure 6: Numerical simulation results of the specimen.

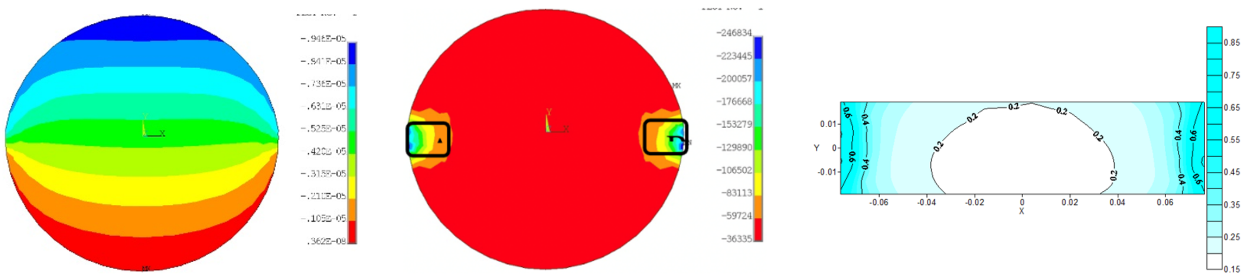

(a) Y-direction displacement cloud when the load is 10 kN

(b) Stress cloud in Y-direction when the load is 10 kN

(c) APPDI3D cloud map when the load is 10 kN

Figure 7: Numerical simulation results of the specimen.

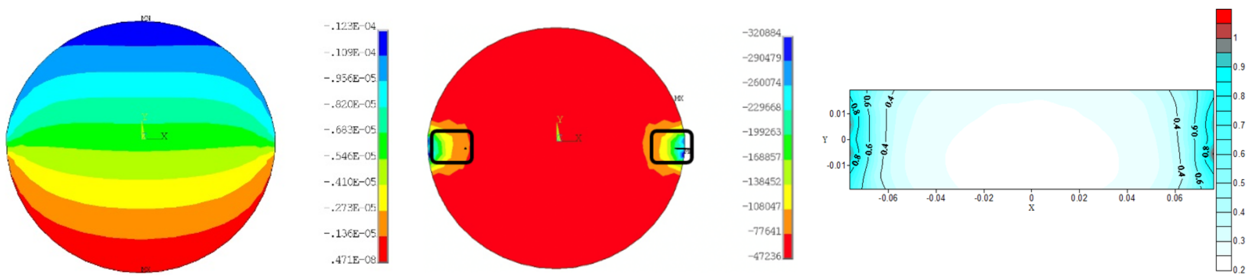

(a) Y-direction displacement cloud when the load is 13 kN

(b) Stress cloud in Y-direction when the load is 13 kN

(c) APPDI3D cloud map when the load is 13 kN

Figure 8: Numerical simulation results of the specimen.

specimen; (c) the figure shows that the maximum value of APPDI in all nodes in the regions A and B is 0.4154, $\sigma_1 = 0.0988$ MPa, $\sigma_3 = 0$ MPa, located in the right side of the specimen (region B). From the analysis of (a), (b) and (c) diagrams, it can be obtained that APPDI is less than 1 under this load, and the numerical specimen is in a safe state.

When the applied load is 6 kN, the Y-direction cloud, Y-direction stress cloud and APPDI cloud of the Marshall specimen are shown in Fig. 6.

Table 4: Marshall test simulation results.

	Specimen size Diameter/mm	High/mm	Applied load F/kN	Cohesion C/Pa	Modulus of elasticity E/Pa	APPDI
Simulation specimens	152.4 mm	95.3	4	0.163E6	681.41E6	0.4200
			6			0.5800
			10			0.8500
			13			1.0000

Figure 6 shows that: when the force is 6 kN, (a) the figure shows that the displacement at the top of the specimen in the Y direction is large and the displacement at the bottom is small, and the cloud is symmetrical, and the maximum displacement is 0.0057 mm; (b) the figure shows that the location where the potential danger points appear in the specimen is in the two regions A and B in the specimen; (c) the figure shows that the maximum value of APPDI in all nodes in the regions A and B is 0.5809, $\sigma_1 = 0.1482$ MPa, $\sigma_3 = 0$ MPa, located in the right side of the specimen (region B). From the analysis of (a), (b) and (c) diagrams, it can be obtained that APPDI is less than 1 under this load, and the numerical specimen is in a safe state.

When the applied load is 10 kN, the Y-direction cloud, Y-direction stress cloud and APPDI cloud of the Marshall specimen are shown in Fig. 7.

Figure 7 shows that: when the force is 10 kN, (a) the figure shows that the displacement at the top of the specimen in the Y direction is large and the displacement at the bottom is small, and the cloud is symmetrical, and the maximum displacement is 0.0094 mm; (b) the figure shows that the location where the potential danger points appear in the specimen is in the two regions A and B in the specimen; (c) the figure shows that the maximum value of APPDI in all nodes in the regions A and B is 0.8524, $\sigma_1 = 0.2471$ MPa, $\sigma_3 = 0$ MPa, located in the right side of the specimen (region B). From the analysis of (a), (b) and (c) diagrams, it can be obtained that under this load, APPDI satisfies $0.5 < \text{APPDI} < 1$, and the numerical specimen is in a safe state.

When the applied load is 13 kN, the Y-direction cloud, Y-direction stress cloud and APPDI cloud of the Marshall specimen are shown in Fig. 8.

Figure 8 shows that: when the force is 13 kN, (a) the figure shows that the displacement at the top of the specimen in the Y direction is large and the displacement at the bottom is small, and the cloud is symmetrical, and the maximum displacement is 0.0123 mm; (b) the figure shows that the location where the potential danger points appear in the specimen is in the two regions A and B in the specimen; (c) the figure shows that the maximum value of APPDI in all nodes in the regions A and B is 1.017, $\sigma_1 = 0.3212$ MPa, $\sigma_3 = 0$ MPa, located in the right side of the specimen (region B). From the analysis of (a), (b) and (c) plots, it can be obtained that under this load, APPDI is close to 1, and the numerical specimen is in the near damage state.

In summary, when the load is 13 kN, the APPDI value of the node appears close to 1 within the range of the bar area from A to B, indicating that the test reaches the plastic zone under this load and imposes in the critical point of damage; when the load is 6 kN, the maximum value of APPDI is 0.5809 within the range of A and B areas, which is close to half of the APPDI value corresponding to 13 kN. When the load is 10 kN, the APPDI value is 0.8524, and when the load is 4 kN, the APPDI value is 0.4154.

4.3.3 Marshall test simulation results and test results comparison analysis

The results of the Marshall test simulations obtained from the above calculations are summarized in Table 4.

Table 4 analysis shows that the material parameter under the load of 13 kN when the Marshall specimen appeared dangerous point, the node Y direction displacement is 0.0037 mm, APPDI value is close to 1, the material reached the critical damage point. Therefore, the material parameters corresponding to the stability of 13 kN, the flow value of 0.0037 mm. consider the fatigue load, when the APPDI value of 0.58, the test specimen force 6 kN that is the fatigue load stability, the flow value of 0.0017 mm. and Guangdong Province, Yunfu to Yangjiang Expressway, Luoding to Yangchun section of the field Marshall indoor test results of 23 mm, the flow value of 0.0017 mm. The stability is 13.09 kN, compared with the test material can meet the pavement structure design requirements.

In summary, the pavement structure is safe under this material parameter. Therefore, it is recommended that the material parameters of the pavement structure of the upper layer: cohesion is 0.1630 MPa, modulus of elasticity is 681.41 MPa, and Poisson's ratio is 0.35.

5. Conclusion

In this paper, APPDI3D was used to evaluate the asphalt pavement structure of Guangle Expressway under the simplified model of three-dimensional bicircular uniform load for mechanical calculation. The damage mode of asphalt pavement of Guangle Expressway under high temperature was analyzed, while the asphalt pavement parameters were optimized and designed, and Marshall finite element test simulation was conducted, and then the results were compared and analyzed with the indoor test results, and the following conclusions were obtained:

1. The analysis results of the simplified model of three-dimensional bicircular uniform load pattern of asphalt pavement of Guangle Expressway under high temperature conditions show that the potential damage pattern of the upper layer of asphalt pavement under high temperature conditions is manifested as

localized rutting damage by TOP-DOWN cracks dominated by tensile stress, and the potential damage pattern of the middle surface layer is manifested as rutting.

2. Under high temperature conditions, the asphalt pavement of Guangle Expressway has potential damage, by adjusting the shear strength parameters of the upper layer of asphalt concrete, the modulus of elasticity is back-calculated, and by comparing the numerical simulation results of the Marshall test with the test results, the stability of the Marshall test is 13 kN, considering the effect of fatigue load, when the APPDI value is 0.58, the stability of the specimen under fatigue load is 6 kN. And the Marshall test flow value of asphalt mixture obtained from the field indoor test is 23 mm and the stability is 13.09 kN, the test material can meet the structural design requirements of this pavement.
3. Comprehensive analysis suggests that the design parameters that should be used for pavement design are cohesion of 0.1630 MPa, modulus of elasticity of 681.41 MPa, and Poisson's ratio of 0.35.

6. Acknowledgment

This research content of this paper is supported by Guangdong Science and Technology Innovation Strategy Special Funds (pdjh2022b0392, pdjh2022b0394) and College Students' innovation and Entrepreneurship Projects (C2106001310, 202211106008).

References

Chen, S. and Sun, Z. (2018). A three-parameter strength theory and its application to brittle materials. *Chinese J. Undergr. Sp. Eng.*, 14:1042–1048.

Cong, Z., Zou, X., and Gong, H. (2013). Influence of heavy load on rutting and fatigue life of asphalt pavement. *J. Wuhan Univ. Technol.*, 35:54–58.

Gao, J., He, T., Huo, Y., Song, M., Yao, T., and Yang, W. (2021). Comparison of modified Mohr-Coulomb model and Bai-Wierzbicki model for constructing 3D ductile fracture envelope of AA6063. *Chinese J. Mech. Eng.*, 34(1):233–245.

Gu, X., Yuan, Q., and Ni, F. (2012). Analysis of influencing factors on asphalt pavement rutting development based on measured load and temperature gradient. *China J. Highw. Transp.*, 25(6):30–36.

Guo, J., Jiang, J., Liu, X., Chen, J., Lu, X., and Yang, Q. (2021). Correction of D-P strength criterion based on elastic strain energy. *J. Civ. Eng.*, 54:110–116.

Guo, J., Liu, X., Huang, W., Luo, X., and Niu, L. (2018). Discussion of Mohr-Coulomb strength criterion based on elastic strain energy. *J. Tongji Univ. (Natural Sci. Ed.*, 46(9):1168–1174.

Hu, C. (2009). Three dimensional finite element analysis of top-down cracking for asphalt pavements. In *Int. Conf. Transp. Eng. 2009*, pages 3248–3253, Reston, VA. American Society of Civil Engineers.

Kabwe, E. (2020). Confining stress effect on the elasto-plastic ground reaction considering the Lode angle dependence. *Int. J. Min. Sci. Technol.*, 30(3):431–440.

Li, M. (2017). Analysis of the fine-scale creep characteristics of asphalt mixtures based on the Drucker-Prager model. *J. North China Inst. Sci. Technol.*, 14:96–100.

Li, Z. and Huang, X. (2017). tudy on improved Mohr-Coulomb model for asphalt paving system of concrete curved slope bridge. *Road Build. Mach. Constr. Mech.*, 34:46–46.

Rukhaiyar, S. and Samadhiya, N. K. (2018). Triaxial strength behaviour of rockmass satisfying Modified Mohr-Coulomb and Generalized Hoek-Brown criteria. *Int. J. Min. Sci. Technol.*, 28(6):901–915.

Schorsch, M. (2003). Effects of segregation on the initiation and propagation of top-down cracks. In *Transp. Res. Board Annu. Meet.*, Washington DC, USA.

Sun, R., Yang, J., Zhao, Y., and Yang, F. (2020). Adaptive upper limit finite element study of higher order units based on Drucker-Prager criterion. *Chinese J. Geotech. Eng.*, 42(2):398–404.

Xie, X., Li, L., Tang, Q., Peng, T., and Luo, C. (2020). Research on shear strength of asphalt mixture based on Moore-Coulomb theory. *J. Hunan Inst. Sci. Technol.*, 41:28–30.

Xu, X. and Wu, C. (2013). Analysis of influence of pavement structural layer parameters on shear stress of asphalt pavement. *Highw. Automob. Transp.*, 4:107–109.